ACS OMEGA

Open Access

http://pubs.acs.org/journal/acsodf

Article

Comparative Analysis of Silk Fibroin Membranes across Cross-Linking Methods: Processing and Characterization

Rocio Gutierrez-Contreras,* Mar Fernandez-Gutierrez, Paula Olalla-Perez, Andres De La Hoz, and Susana Marcos

Cite This: *ACS Omega* 2024, 9, 38452−38461

Read Online

ACCESS | Metrics & More | Article Recommendations | Supporting Information

ABSTRACT: Silk fibroin (SF) extracted from silkworm silk can be transformed into transparent membranes with well-suited physical properties for ophthalmic applications. There is ample literature on the fabrication and characterization of SF-based membranes; however, the use of diverse SF extraction protocols and characterization methods or their settings makes it difficult to compare different silk membrane properties across studies. In this work, we fabricated 10 families of SF-based membranes by physical cross-linking and one non-cross-linked as a control. We evaluated transparency (ranging from 84.5 to 95.3% in the visible spectrum), enzyme stability (from 24 h to 200 days in protease XIV), decomposition temperature (280−290 °C), water uptake (40−60%), Young's modulus (8−30 MPa), roughness (1.6−22.7 nm), and FTIR spectra for the secondary structure. We found correlation between water uptake and the Young's modulus (the lower the water uptake, the higher the Young's modulus) and a relationship between membrane stability in protease XIV and the secondary structure of the proteins. Higher surface roughness and faster degradation were found in membranes cross-linked with polyethylene glycol, and conversely, lower roughness and lower degradation were found in methanol, ethanol, or isopropanol crossed-link membranes. This ample compilation of materials and their characterization will aid in the selection of a SF-based material according to the needs of the application.

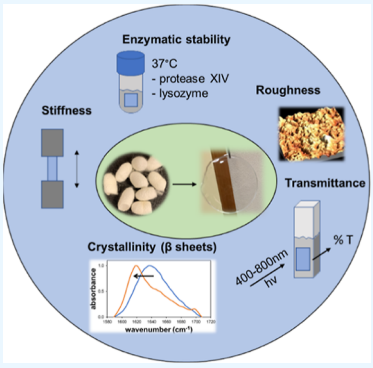

1. INTRODUCTION

In recent years, silk fibroin (SF) materials have been developed for a wide range of applications, including tissue engineering, drug delivery,[1,2] food industry,[3,4] and electronic components.[5]

The versatility of SF as a biomaterial comes from its biocompatibility, low immunogenicity, ease of use in various formats,[6,7] tunable mechanical properties, and lightweight. SF is an FDA-approved biomaterial, and there are several SF-based medical products commercially available, two of them with particular interest in the eye care market such as silk-containing eye drops (SilkTears by SilkTech) and silk sutures (Sofsilk by Medtronic).

To our knowledge, there is no SF-based product in the form of films or membranes in ophthalmology, although SF-based systems have been proposed as efficient biopolymers for wound dressings, corneal and drug delivery systems, and corneal tissue engineering.[8−10] The possibility of achieving a high degree of transparency, in combination with the above-mentioned advantages, makes SF-based membranes highly promising for use in ophthalmology. A drawback that may have prevented a more widespread use of these biopolymers in ophthalmology is the high variability and dependence of their properties on the specifics of numerous manufacturing steps.

The manufacturing of silk membranes involves production of silk, extraction, casting, and cross-linking of the SF. Each of these steps plays a role in determining the physical and structural properties of the resulting SF-membranes. SF obtained from the silkworm (*Bombyx mori*) cocoons is conditioned to the worms' diet, stifling method, age of the cocoons, and SF extraction method, including the degumming time, which affect the biopolymer and its properties, making standardization important to increase guarantee reproducibility.[11−16] The degumming process has been shown to play an important role in the properties of the material made with regenerated SF.[14,16] For this reason, we have produced all the materials from the same silk batch following the same processing method, which involved a degumming time of 40 min. SF membranes are typically cast from the SF solution. To maximize the reproducibility of the resultant membranes, casting should be carried out under standard temperature and humidity conditions in a mold with set dimensions. The final step in the production of SF membranes is cross-linking to achieve their insolubility in water. This can be performed through physical cross-linking, which induces beta-sheets, or through covalent cross-linking. Physical cross-linkers include

Received: March 6, 2024
Revised: July 29, 2024
Accepted: July 31, 2024
Published: August 30, 2024

Table 1. Methods to Produce the Membranes of the Study

sample	[SF] [% (w/v)]; volume (mL)	membrane casting	cross-linking method	refs
SF membrane control (SFC)	6%; 6 mL	SF solution stirred with water at 300 rpm followed by direct cast in a Petri dish		
SF cross-linked with methanol (SFM)	6%; 6 mL	SF solution stirred with water at 300 rpm followed by direct cast in a Petri dish	immersion of the membrane in 75% methanol for 15 min	
SF cross-linked with ethanol (SFE)	6%; 6 mL	SF solution stirred with water at 300 rpm followed by direct cast in a Petri dish	immersion of the membrane in 70% ethanol for 20 min	
SF cross-linked with isopropanol (SFI)	6%; 6 mL	SF solution stirred with water at 300 rpm followed by direct cast in a Petri dish	immersion of the membrane in 70% isopropanol for 20 min	
SF membrane cross-linked with PEG 300 (SFP)	3%; 6 mL	in a Petri dish, after mixing with the cross-linker	(1) 3% SF solution stirred with 5% PEG (v/v) at 700 rpm for 2 min (2) add 0.6 mL water and cast the solution (3) after casting, wash the membrane in water overnight, to remove the PEG	adapted from ref 32
SF membrane cross-linked with PEG 300 and immersed in methanol (SFPM)	3%; 6 mL	in a Petri dish, after mixing with the cross-linker	(1) prepare a SFP membrane, without removing the PEG (2) soak the SFP membrane in 75% methanol for 15 min. Leave the membrane to dry overnight (3) wash the membrane overnight to remove the PEG	adapted from ref 32
SF membrane cross-linked with PEG 300 and immersed in ethanol (SFPE)	3%; 6 mL	in a Petri dish, after mixing with the cross-linker	(1) prepare a SFP membrane, without removing the PEG (2) soak the SFP membrane in 70% ethanol for 20 min. Leave the membrane to dry overnight (3) wash the membrane overnight to remove the PEG	adapted from ref 32
SF membrane cross-linked with PEG 300 and immersed in isopropanol (SFPI)	3%; 6 mL	in a Petri dish, after mixing with the cross-linker	(1) prepare a SFP membrane, without removing the PEG (2) soak the SFP membrane in 70% isopropanol for 20 min. Leave the membrane to dry overnight (3) wash the membrane in water overnight to remove the PEG	adapted from ref 32
SF membrane cross-linked with glycerol (SFG)	6%; 6 mL	in a Petri dish, after mixing with the cross-linker	(1) stir the SF solution with 5% (w/w) glycerol at 700 rpm for 2 min (2) after casting, wash the membrane in water overnight to remove the glycerol	33
SF membrane cross-linked with glycerol and PEG 300 (SFGP)	6%; 6 mL	in a Petri dish, after mixing with the cross-linker	(1) stir the SF solution with 30% (w/w) glycerol solution at 200 rpm for 15 min (2) add PEG 80% (w/w) to the previous solution and stir at 700 rpm for 2 min. The mass ratio of SF/PEG/Gly should be 10:5:3 (3) wash the membrane in water overnight to extract the PEG and glycerol	34
SF membrane water annealed (SFWA)	6% SF; 6 mL	SF solution directly in a Petri dish with the lid on		

https://doi.org/10.1021/acsomega.4c02204
ACS Omega 2024, 9, 38452−38461

methanol, ethanol, isopropanol, glycerol, polyethylene glycol (PEG), and annealing methods (slow, controlled evaporation of the water in the cast solution). The polar groups in PEG, glycerol, methanol, ethanol, and isopropanol attract water present in the SF and induce the transition from random coil to beta sheets.[17,18] Covalent cross-links are produced by enzymes or photo-oxidization.[19] In this study, we describe the production and characterization of SF-membranes obtained from silkworm cocoons (*B. mori*) produced by different physical cross-linking methods. We assess the amino acid composition of SF,[20,21] and the transparency,[10,22,23] crystallization,[18,24,25] tensile strength,[26,27] surface roughness,[28] enzymatic[10,29,30] and thermal[27] stability, and water uptake of the different cross-linked membranes. We hypothesize that materials with higher crystallinity will have a slow degradation over time and higher Young's modulus. On the other hand, materials cross-linked with PEG, a porogen, may have rough surfaces and have a higher water uptake. Roughness is an important parameter to measure, as SF-based membranes may be used as scaffolds or substates for cell culture. Rough surfaces have been shown to be more conductive to cell proliferation and growth.[28]

Although there is ample literature on the production of SF-based biomaterials and their characterization,[6,7,9,31] a comparison across studies is highly limited by the differences in raw material (which may affect the amino acid proportion), processing, and characterization techniques.

In this study, we present a direct comparison of the properties of SF membranes, obtained from silk from cocoons of same silkworm species, provider, and batch and extracted through a single protocol and under the same conditions. All membranes were cast with water-based solvent, as a more affordable and innocuous solvent compared to formic acid or hexafluoroisopropanol (HFIP). Certain SF-based materials cast with formic acid or HFIP have shown to have superior mechanical properties, compared to materials cast with water-based solvents.[10] However, we focused on greener protocols for SF fabrication.

As all the materials were made under the same conditions, the properties of the SF membranes fabricated and characterized in this work can be directly compared across cross-linking methods, ensuring that the rest of the influencing parameters are constant. This study fills a gap in the literature where manufacturing conditions are either not reported in detail or differ across studies, making a direct comparison unfeasible. We have focused on SF membranes for potential use as biomedical materials, in particular, for ophthalmological applications. To our knowledge, this is the first report offering a detailed account of the SF membrane manufacturing process, with comprehensive stability, structural, topographical, mechanical, and optical characterization of the properties of a broad number of different membranes. In total, ten membranes (and a control without cross-linking) were obtained through different cross-linking procedures and with a water-based solvent, facilitating the selection of the most suitable membranes for a given target application.

2. MATERIALS AND METHODS

2.1. Materials and Reagents. Silk cocoons were produced by silkworm *B. mori* at Instituto Murciano de Investigación Agraria y Medioambiental (IMIDA) (Murcia, Spain). Sericulture at IMIDA is performed under fully standardized conditions both before and during cocoon formation.

Sodium carbonate anhydrous 99.5% with a laboratory reagent grade and lysozyme were supplied by Thermo Fisher Scientific. Polyethylene glycol (PEG) 300 for synthesis, PBS in tablets, lithium bromide ReagentPlus (R) > 99%, protease from *Streptomyces griseus* type XIV ≥ 3.5 units/mg solid powder, methanol for HPLC ≥ 99.9%, and ethanol were supplied by Merck. Glycerol 99.0% was purchased from Panreac. Isopropanol 70% was provided by Alcoholes Montplet, S.A.U. Dialysis membrane MWCO 3.5 kDa was supplied by Spectrum Chemical.

2.2. Preparation of SF Solution. SF was prepared based on a previously published method[6] with the following adjustments and specifications: degumming time was 40 min; the degummed SF fibers were allowed to dry at 60 °C overnight; SF in LiBr solution was stirred twice with a spatula throughout the 4 h at 60 °C to ensure complete dissolution of SF in the LiBr solution; the final solution was dialyzed in a 16 cm membrane, folded three times on each side, and clamped; the resulting SF solution was centrifuged at 7830 rpm for 1 h at 4 °C to remove impurities.

Final SF concentration (6−7% w/v) was calculated by weighing 0.5 mL of the SF solution before and after drying at 60 °C.

The amino acid composition of the SF batches used to produce the membranes was analyzed as a quality control, in order to ensure that the raw SF used in all membranes was identical with regard to the amino acid profile. The samples were hydrolyzed with 6 N HCl at 110 °C for 24 h under vacuum conditions. The analyses were performed on a Biochrom 30 amino acid analyzer (Biochrom Co., Cambridge, UK). The separation of amino acids was carried out by ion exchange chromatography and postcolumn derivatization with ninhydrin. Calibration was performed using the AAS18 amino acid standard purchased in Merck.

2.3. Preparation of SF Membranes. All films were prepared with SF solution, and different cross-linking methods were used to enhance crystallinity in the membranes. Control membranes were also prepared without any cross-linking process.

Membranes were cast in 90 mm diameter polystyrene Petri dishes. Unless specified, the Petri dishes were used lid-less. The casting was carried out in a climatic chamber (Memmert HPP 260 eco) at 25 °C and 40% relative humidity, placing the Petri dish on an orbital shaker at 40 rpm overnight, with the exception of the SF water annealed (SFWA) membranes, in which full evaporation takes longer. The different procedures used to prepare the membranes in the current study are listed in Table 1.

2.4. Transparency of the Films. Transmittance measurements in the visible range (400−800 nm) were performed using a UV−vis−NIR spectrophotometer (Cary 5000, Agilent). Film strips were placed vertically inside polystyrene cuvettes with water, ensuring the transmission of the spectrophotometer light beam through the sample. Five strips were taken from each membrane and measured. The transmittance of each strip was calculated from the average of the data points obtained in the 400−800 nm range, measured in 1 nm steps. Afterward, the transparency of each film was set as the transmittance average of the 5 strips.

2.5. Enzyme Stability of the Films and Water Uptake. For ophthalmology applications, the membranes should be

https://doi.org/10.1021/acsomega.4c02204
ACS Omega 2024, 9, 38452−38461

tested for stability in the tear fluid. Tear is composed of different proteins and lipids, with a formulation that to date has not been possible to replicate synthetically. Different tear like fluids (TLFs) have been proposed. A standard protocol is described by ref 35, which uses guidelines provided by Johnson and Johnson Vision Care, Inc. (JJVCI; Jacksonville, FL, USA). The protocol included lysozyme as one of the TLF components. In this study, we have tested the membranes' stability with the weight loss method by immersing the materials in PBS, lysozyme, and protease XIV media, which is typically used as a positive control in material degradation assays, due to hydrolytic activity.[29] Water uptake at 24 h was also assessed.

Enzymatic degradation studies were carried out at 37 °C. Protease XIV (0.05 U/mL) and lysozyme (500 U/mL) solutions were prepared in PBS buffer (pH 7.4). Five samples of 1 cm^2 of each film were tested per condition. All media were changed twice a week.

Excess media were removed from the films with a paper towel before weighing them.

Enzymatic degradation was assessed as weight loss of the sample after different times in each media, using the following equation[10,36]

$$\% \text{ weight loss} = [(M_t - M_d)/M_t] \times 100$$

where M_t is the mass of the sample after 24 h in the PBS, lysozyme, or protease solution, and M_d is the mass of the sample after being removed from the PBS, lysozyme, or protease solution at different times.

Water uptake percentage was calculated using the following equation

$$\% \text{ water uptake} = [(M_t - M_0)/M_0] \times 100$$

where M_t is the mass of the sample after 24 h in PBS, lysozyme, or protease solution, and M_0 is the initial dry mass measured before immersing the sample in the different media.

2.6. Mechanical Properties. The Young's modulus of the SF membranes was evaluated using strip extensiometry (UStretch uniaxial tensile testing device, CellScale, Waterloo, ON, Canada). Strips of 15 mm length and 5 mm width were cut from each SF membrane, and their thickness was recorded (40−100 μm). The samples were mounted in the stretcher and allowed to hydrate for 10 min prior to the start of the test. Testing was conducted in a water bath. Samples were stretched in three steps. The first two steps consisted of a strain of 1% per second applied during 10 s and then a return to zero strain. The final step consisted of a strain of 1% per second applied until the breakage of the sample. The Young's modulus as well as elongation at break, toughness, and ultimate tensile strength were calculated from the final step. Young's modulus was calculated from the first 10% of strain.

2.7. Fourier Transform Infrared Spectroscopy. The crystallization of the SF membranes was evaluated using a FTIR spectrophotometer (ALPHA II, Bruker Optics GmbH & Co), coupled with a diamond crystal Attenuated Total Reflection (ATR) accessory. The material absorbance was collected from 400 to 4000 cm^{-1} with a resolution of 4 cm^{-1} and 128 scans. Each membrane was measured in five different spots. The secondary structure of the SF membranes was analyzed following previously described protocols.[24,25,37] The amide I region (1588−1708 cm^{-1}) was selected, and a linear baseline was applied to the spectrum. Deconvolution of the amide I region was performed using the second derivative analysis, with a third-degree polynomial function and a nine-point Savitzky−Golay smoothing filter. The local minimums were determined in the second derivative. These points were fixed on the amide I spectra for deconvolution, whereas the widths and heights were allowed to vary. Curve fitting was carried out with a Levenberg−Marquardt algorithm function, assuming Lorentzian shapes to the deconvoluted peaks. The percentage of the secondary structure was calculated by integrating the area of each deconvolved curve and normalizing to the total area of the amide I band. The assignation of the bands to the different secondary structures was set following the literature.[24]

Independently from the deconvolution process, for visualization purposes, all of the spectra from each membrane were normalized to their maximum intensity and averaged to obtain a single spectrum per membrane. All data processing was carried out with OriginLab software.

2.8. Surface Roughness. Surface topography tests were performed on an atomic force microscope (AFM), Multimode SPM, (Veeco Instruments, USA) with an EV-scanner under ambient condition. Three samples of each membrane were measured. Samples were hydrated in water and attached to the AFM holder using double-sided tape and allowed to evaporate. This mounting procedure resulted in a flat surface. The images were taken in tapping mode. A resonance frequency of around 300 kHz, very close to the resonance frequency of the tip, was kept constant between the tip and the sample. Measurements and images were processed with WSxM 5.0 software.[38]

2.9. Thermostability Analysis. Thermal gravimetric analysis (TGA) was carried out in a TA-Q500 system (TA Instruments, USA). One sample per membrane was measured. Samples were heated from room temperature to 800 °C under a nitrogen atmosphere at a 10 °C/min heating rate. TA Instruments Universal Analysis 2000 software was used to analyze the thermograms obtained in the measurements and calculate the decomposition temperature of SF in the different films.

2.10. Statistical Analysis. Measurement error was quantified as the standard deviation of measurements on different regions of the same membrane (n = 5 for transparency, enzymatic stability, and FTIR analysis; n = 3 for AFM data). Analysis of variance (ANOVA) was used to assess the statistically significant differences among the different types of membranes.

3. RESULTS

We present structural, stability, topographical, mechanical, optical, and thermal properties of a total of ten SF-based cross-linked membranes, obtained from a single batch of silk cocoons, from which SF is subsequently extracted.

3.1. Amino Acid Composition Analysis. The amino acid composition in three different batches of SF (worms cultivated at different time frames under the same conditions) shows similar amino acid proportions, as seen in Figure 1 and Table 2. In particular, we found less than 0.4% intersample variability in glycine (which makes up to 44% of the amino acid composition), 0.7% in alanine (30.1% of the total), and 4.5% serine (10.7% of the total).

3.2. Transparency of the Films. All ten samples of membranes following different cross-linking methods (n = 5 per method) have an 84.5−95.3% transmittance in the visible spectrum, as seen in Table 3 and Figure S1. Transmittance measurement variability ranged from 0.4 to 11.2%. ANOVA

https://doi.org/10.1021/acsomega.4c02204
ACS Omega 2024, 9, 38452−38461

Table 2. Amino Acid Composition of SF (n = 3 Batches)

amino acid	composition (% nmol)
Gly	44.0 ± 0.2
Ala	30.1 ± 0.2
Ser	10.7 ± 0.5
Tyr	5.3 ± 0.1
Val	2.2 ± 0.1
Asp	1.7 ± 0.0
Glu	1.1 ± 0.0
Thr	0.9 ± 0.0
Phe	0.7 ± 0.1
Ile	0.6 ± 0.0
Pro	0.5 ± 0.1
Leu	0.5 ± 0.0
Arg	0.5 ± 0.0
Cys	0.4 ± 0.1
Lys	0.3 ± 0.0
His	0.2 ± 0.0
Met	0.1 ± 0.0

Table 3. Transmittance of the Materials in the 400−800 nm Range (n = 5 per Material)

material	transmittance (%)
SFM	92.1 ± 1.6
SFE	93.5 ± 1.4
SFI	89.2 ± 3.5
SFP	94.6 ± 1.6
SFPM	91.7 ± 2.3
SFPE	92 ± 2.8
SFPI	95.3 ± 0.4
SFG	84.5 ± 9.4
SFGP	91.8 ± 3.8
SFWA	89.4 ± 11.2

analysis with Tamhane test shows that there are no significant differences among the materials (p < 0.05).

3.3. Enzymatic Stability of the Films. Membranes show no weight loss over time in PBS or lysozyme media. However, at times over 100 days, membranes cross-linked with glycerol (SFG); PEG (SFP); and PEG + alcohols (SFPM, SFPE, SFPI and SPGP) break apart. In protease media, this behavior is observed after less than 24 h in protease. Water annealed membranes (SFWA) last for 72 h in protease before breakage. Membranes cross-linked with ethanol, isopropanol, or methanol (SFE, SFI, SFM, respectively) present a slow and sustained weight loss for over 200 days (Figure 2). In the first days, there is a high density of data points, as the materials were weighted every day.

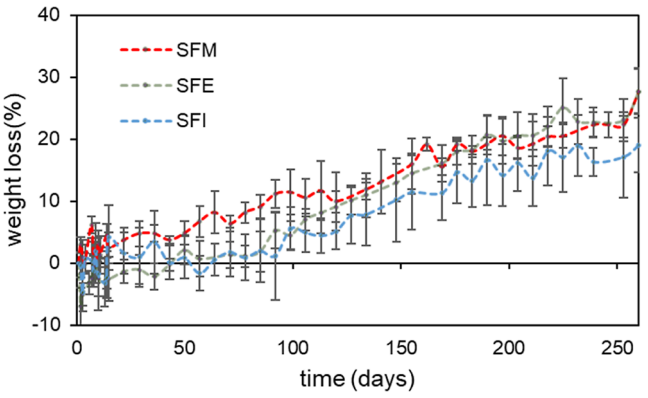

Figure 2. Average weight loss of SFM, SFE, and SFI over time in protease XIV.

In general, SF membranes cross-linked with ethanol, isopropanol, methanol, or water annealed (SFE, SFI, SFM, and SFWA respectively) show the lowest water uptake, around 40%. Membranes cross-linked with glycerol (SFG); PEG (SFP); and PEG + alcohols (SFPM, SFPE, SFPI and SPGP) show water uptake above 60% in PBS and lysozyme. ANOVA with Tamhane test show that membranes cross-linked with PEG and membranes cross-linked with alcohols are statistically different (p < 0.05) in both media.

3.4. Mechanical Properties. Figure 3A and Table 4 show the Young's modulus (uniaxial testing) of all tested membranes. Stress−strain plots are shown in Figure S2. Young's modulus expands from 8 to 30 MPa, with average standard errors of 0.7 MPa. ANOVA was conducted to assess the differences among the mean stiffness values across groups. The results revealed a significant effect of cross-linking (p < 0.05). Membranes cross-linked with glycerol show the lowest Young's modulus, and those cross-linked with methanol, ethanol or isopropanol show the highest Young's modulus. The presence of PEG (which acts as a porogen) decreases stiffness by 50% on average (in comparison with the corresponding membranes with methanol, ethanol or isopropanol cross-linking but not PEG).

Figure 3B shows the relationship between the average water uptake in each membrane after 1 h in PBS and its Young's modulus. The Young's modulus decreases as water uptake increases, as expected.[27] Membranes that have been cross-linked with PEG have a larger superficial surface and therefore

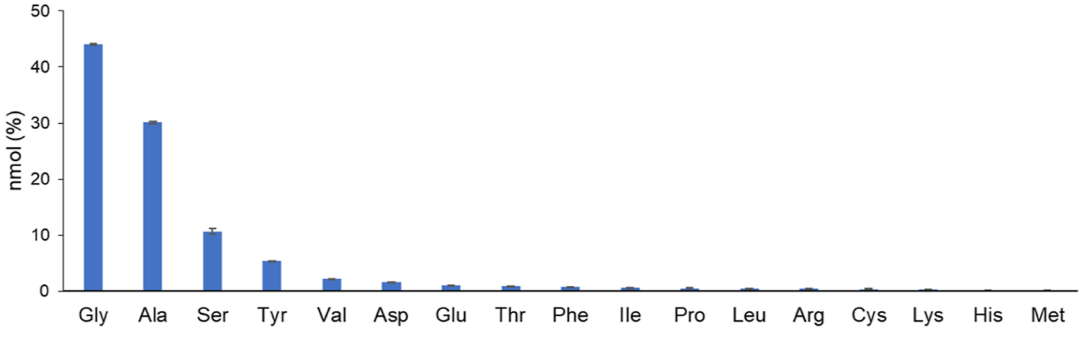

Figure 1. Amino acid composition of SF (n = 3 batches).

https://doi.org/10.1021/acsomega.4c02204
ACS Omega 2024, 9, 38452−38461

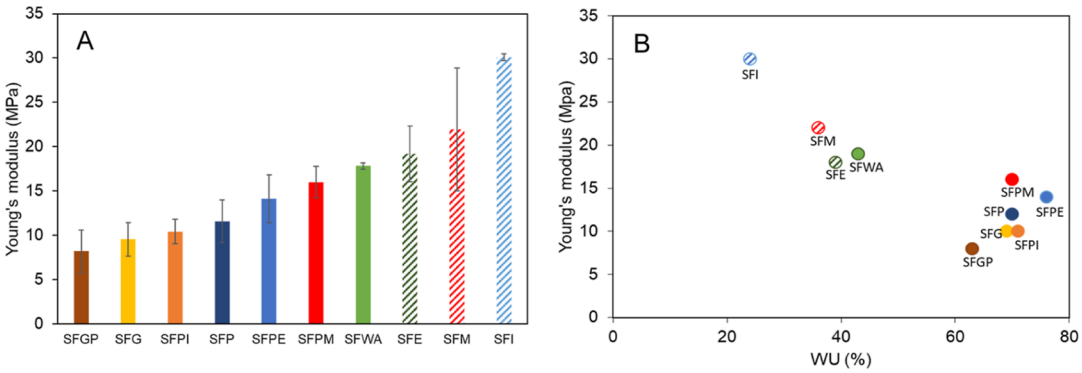

Figure 3. (A) Young's modulus of the cross-linked membranes. (B) Young's modulus vs water uptake (1 h in PBS).

Table 4. Young's Modulus, Elongation at Break, Toughness, and Failure Stress of Strips of the SF-Based Materials (n = 2−7 per Material)

material	Young's modulus (MPa)	elongation at break (%)	toughness (MPa)	failure stress (MPa)
SFI	30.1 ± 0.4	132.8 ± 47.1	5.6 ± 2.6	5.6 ± 1.1
SFM	21.9 ± 6.9	39.4 ± 14.2	0.7 ± 0.3	2.5 ± 0.3
SFE	19.2 ± 3.2	134.2 ± 69.3	3.9 ± 2.4	3.4 ± 1.0
SFWA	17.8 ± 0.4	24.8 ± 12.6	0.4 ± 0.3	2.3 ± 0.1
SFPM	16.0 ± 1.8	22.8 ± 3.2	0.3 ± 0.0	1.8 ± 0.0
SFPE	14.1 ± 2.7	47.1 ± 16.3	0.7 ± 0.1	2.0 ± 0.3
SFP	11.6 ± 2.4	84.4 ± 33.0	1.7 ± 1.1	2.4 ± 0.6
SFPI	10.4 ± 1.4	101.5 ± 38.1	1.5 ± 0.8	1.7 ± 0.3
SFG	9.6 ± 1.9	151.3 ± 81.3	2.4 ± 1.5	1.9 ± 0.7
SFGP	8.2 ± 2.4	181.8 ± 10.8	2.4 ± 0.8	1.8 ± 0.6

are more prone to absorb water, increasing their water uptake. Besides, the higher water uptake in membranes cross-linked with PEG is likely associated with lower compactification due to the presence of pores, which in turn also results in a decrease of Young's modulus.

Table 4 also shows the elongation at break, toughness, and failure stress of the silk membranes. On average, the membranes cross-linked with ethanol, methanol, and isopropanol have higher values than those cross-linked with other methods. However, contrary to the Young's modulus, membranes cross-linked with glycerol showed the highest elongation-at-break. There is higher standard deviation in the data, likely due to small imperfections in the SF strips affecting the elongation at break.

3.5. FTIR Study. FTIR spectra show band shifts in the cross-linked membranes. Figure 4A shows the spectra of the amide I band (1588−1708 cm^{-1}) of all of the membranes. In the non-cross-linked membrane (SFC), the amide I band is centered at 1636 cm^{-1} and shifts to 1620 cm^{-1} in the cross-linked membranes. This shift is attributed to a change from random coil to beta sheets.[24,25] Membranes cross-linked with PEG or glycerol (SFP, SFPM, SFPE, SFPI, SFG, and SFGP) show bands (1636; 1646; 1652 cm^{-1}) in the random coil region. These bands are not present or are not as intense in the spectra of the membranes cross-linked with methanol, ethanol, or isopropanol (SFM, SFE, SFI), nor in that of the SFWA. Figure 4B shows the percentage of secondary structures of different SF-based membranes. Detailed data, vibrational band assignments, and deconvolved bands are shown in Table S1 and Figure S3, respectively. ANOVA with Tamhane test shows that SFG, SFC, SFM, SFE, and SFI have statistically different proportions of random coil; SFC, SFG, SFE, and SFI do also show statistically different proportions of beta sheets (p < 0.05).

3.6. Surface Roughness. The membrane surface roughness was investigated by AFM. R_q (geometric average roughness) and R_a (average roughness parameter) values are shown in Table 5. Figure 5 shows the AFM images of small areas of the surface (2 μm across) and roughness values (R_q) for all membranes. Control (non-cross-linked, SFC), water annealed (SFWA) and membranes cross-linked with methanol, ethanol, or isopropanol (SFM, SFE, SFI) showed the lowest roughness, while the membranes in which PEG was used as a cross-linker and porogen showed a 5−14-fold increase in surface roughness. Three samples were measured for each material, and the results were expressed as mean ± standard error of the mean.

3.7. TGA Analysis. TGA thermograms and DTG (Figure S4) show low mass loss up to 200 °C, attributed to loss of water and volatile molecules, and a high mass loss between 200

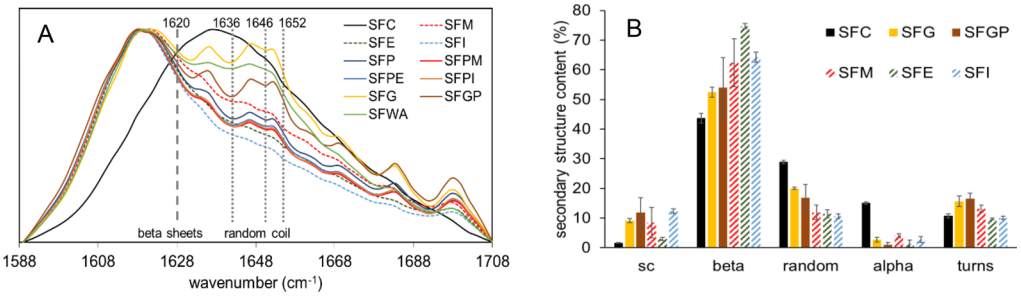

Figure 4. (A) Amide I FTIR spectra of all of the membranes. Vertical dashed line indicates the β sheet band at 1620 cm^{-1}, and the vertical dotted lines indicate the random coil bands at 1636, 1646, and 1652 cm^{-1}. (B) Secondary structure of membranes SFC, SFG, SFGP, SFM, SFE, and SFI.

https://doi.org/10.1021/acsomega.4c02204
ACS Omega 2024, 9, 38452−38461

Table 5. R_a and R_q Values of all the Materials (n = 3 per Material)

material	R_a (nm)	R_q (nm)
SFC	3.0 ± 0.8	3.1 ± 0.0
SFWA	2.7 ± 0.2	3.5 ± 0.3
SFM	1.7 ± 1.0	1.6 ± 0.4
SFE	6.1 ± 0.7	7.7 ± 0.6
SFI	1.9 ± 0.4	2.6 ± 0.4
SFP	17.3 ± 1.9	22.7 ± 1.4
SFPM	10.5 ± 1.2	13.1 ± 1.4
SFPE	13.2 ± 1.3	16.7 ± 1.3
SFPI	9.2 ± 1.3	11.8 ± 1.4
SFG	15.1 ± 2.0	18.4 ± 2.7
SFPG	6.5 ± 0.6	9.5 ± 0.6

and 500 °C, attributed to decomposition of the samples, similar in all membranes. Similarly, the calculated decomposition temperature of the membranes is between 280 and 290 °C, regardless of the manufacturing or cross-linking procedure.

4. DISCUSSION

We described and characterized the production of SF from silkworm (*B. mori*) and studied the cross-linked membranes through different methods.

4.1. SF Solution Analysis. As a quality control measure for the SF used to produce the membranes, the assessment of the amino acid composition of SF showed a homogeneous composition across different SF batches. The quality of the silk could vary across silkworm breed, diet, and ambient conditions, which are controlled before and during cocoon formation.

Published amino acid analysis of the SF show relative variations in the proportion of glycine, alanine, and serine across studies.[20,21] However, the three SF batches analyzed in this study show a high degree of consistency in the relative distributions of these amino acids. We propose the use of SF amino acid analysis as a quality control for the SF solutions, as different silk cocoon batch and sources may differ in composition, likely affecting the properties of the manufactured membranes and becoming a potentially high source of variability.

4.2. Optical Properties. Transparency, generally an important feature for ophthalmic applications, is a common characteristic across all produced membranes. The transmittance measurement variability, ranging from 0.4 to 11.2%, may be due to variations in the membrane thickness, particularly in the SFWA and SFG materials, which show the highest variability (11.2 and 9.4%, respectively). Membranes cross-linked with methanol, ethanol, or isopropanol, besides being stable materials throughout time in protease (positive control), maintain their transparency in PBS for over a year.

4.3. Degradation and Mechanical and Structural Properties. SF is not considered a biodegradable material by the US Pharmacopeia's definition, although the literature suggests it is.[30] As in previous reports, we found that the degradation properties vary substantially with the degrading enzyme. All of the membranes remain stable in PBS and lysozyme, without weight loss over time. Membranes cross-linked with glycerol (SFG); PEG (SFP); and PEG + alcohols (SFPM, SFPE, SFPI, and SPGP), break apart after a period of 100 days in these media. In SFM, SFE, or SFI, the membranes remained intact (no breakage) at the end of the examination experiment, which extended for over 200 days. The behavior in the protease was different between both sets of materials. SFG, SFP, SFPM, SFPE, SFPI, and SPGP broke apart after less than 24 h in protease. However, SFM, SFE, and SFI have a continuous weight loss over time. Very likely, this effect arises from a less prominent crystalline structure in the SFG, SFP,

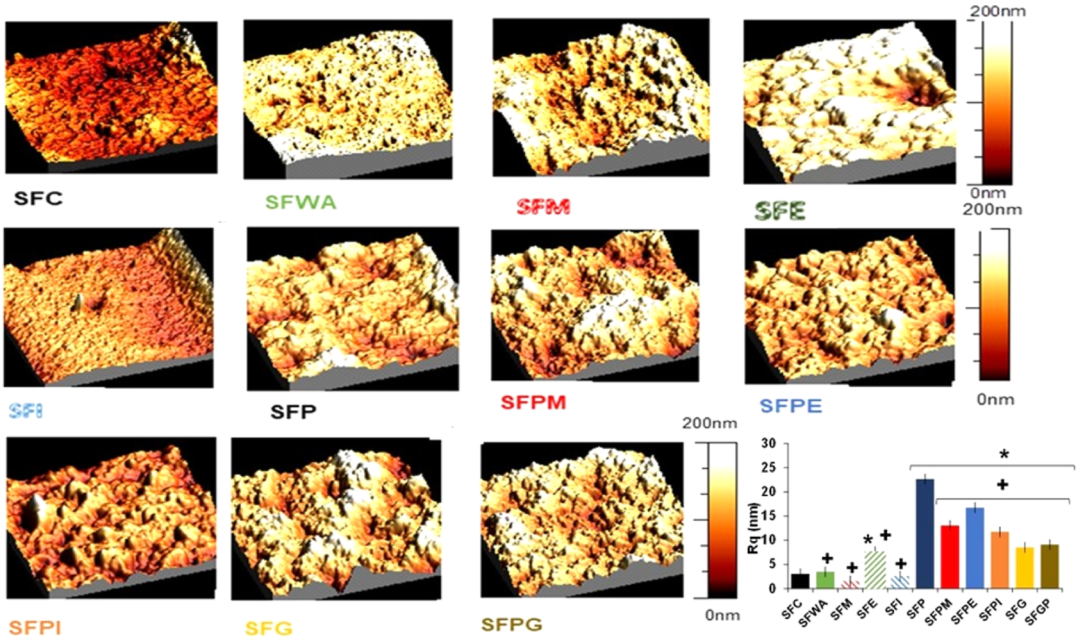

Figure 5. AFM images (2 × 2 μm^2) of the surfaces of all the membranes; surface roughness of membranes estimated from AFM images (bottom right bar plot). Bars represent mean surface roughness (n = 3) and error bars represent the standard error of the mean. Statistical analysis was performed by one-way ANOVA with Tukey's test to determine the statistical significance of the results. *p < 0.05, for statistically significant samples vs the control (SFC), and ^{+}p < 0.05, for statistically significant samples vs the SFP membrane.

https://doi.org/10.1021/acsomega.4c02204
ACS Omega 2024, 9, 38452−38461

SFPM, SFPE, SFPI, and SPGP membranes, seen in the FTIR spectra, enhancing the accessibility to water and protease solved in it.[29,39] Membranes obtained by water annealing present a more crystalline structure[40,41] as seen in our FTIR data, which may explain the 72 h (instead of 24 h) time before breakage in protease. The secondary structure of membranes cross-linked with glycerol and PEG shows a higher proportion of the random coil structure than membranes cross-linked with methanol, ethanol, or isopropanol. This is in consonance with the higher beta sheets proportion of the latter. As reported in the literature, protease degrades first the amorphous structures of SF and then the crystalline ones.[29] This may explain the sustained, constant weight loss of SFM, SFE, and SFI over time in protease, which may be degrading the amorphous structures over time. However, given the higher proportion of beta sheets, the crystalline structure may prevent the materials from breaking, as it occurs with the materials cross-linked with PEG, glycerol, or water annealed. As a side note, the SFG membranes in our study were cast with 5% (w/w) glycerol and the resulting membrane did not dissolve when hydrated, contrary to the previously published results,[33] where membranes cast with 2−5% (w/w) glycerol dissolved upon water immersion. This difference may be due to stirring speed and time during the mixing of SF with glycerol, which may promote the formation of beta-sheets.

Comparison of enzymatic degradation results with the literature is challenged by differences in the protease concentrations, differences in sample surface size, and variations in the protocols. Degradation is generally calculated by weight difference, so slight weight changes can result in high water uptake variability. We minimized the variability by always measuring in the same conditions with the same experimenter.

We have shown that Young's modulus decreases upon the water uptake capacity of the membrane. This is likely the result of mechanical properties being affected by water hydration[27,42,43] and, more substantially, by the presence of pores that appear to decrease the stiffness of the membranes. Also, the FTIR results show the increase in crystallinity and beta sheets in the cross-linked membranes, as expected. Membranes with pores present a rougher surface than those of the membranes that were not cross-linked with PEG, as confirmed by AFM.

Young's modulus measurements are also subjected to protocol variations across studies, among others, whether they are performed in dry or hydrated conditions. Samples in this study were tested under hydration conditions. In general, our data for Young's modulus are comparable with the data published in the literature (within the same order of magnitude). For example, Young's modulus for SFG was 9.6 ± 1.9 MPa in ref 33 and 5.2 ± 0.6 MPa in our study; for SFP, it was 10 MPa[44] in a similar membrane and 11.5 ± 2.4 MPa in our study; for SFM and SFWA reports,[27] the values were 18.70 ± 6.98 MPa and 21.97 ± 1.52 MPa, and 21.9 ± 6.9 MPa and 17.8 ± 0.37 MPa in our study, respectively.

Amide I FTIR spectra show the expected increase in crystallinity after cross-linking,[18,24,45] shifting from 1636 in the random coil region to 1620 cm^{-1} in the beta sheets region. Membranes cross-linked with PEG and/or glycerol, in addition to the band at 1620 cm^{-1}, show smaller bands at 1636; 1646; and 1652 cm^{-1} in the random coil region, which are not present in the membranes cross-linked with methanol, ethanol, or isopropanol. This indicates that the secondary structure of the membranes cross-linked with methanol, ethanol, or isopropanol have a higher proportion of beta sheets than the ones cross-linked with PEG and/or glycerol, as seen in the secondary structure analysis. This is in correspondence with the water uptake and Young's modulus, as beta sheets are hydrophobic domains, which decrease the permeability of the membranes in water and enhance their mechanical properties.

These results can guide decisions regarding the type of the SF-based material needed for different ophthalmological applications. For example, water uptake is an important feature in contact lenses, which could be made of SF. Furthermore, our material degradation results are relevant for disposable contact lenses and tune them to their wear time regimes (daily, monthly, etc...), as well as for applications as contact lens bandages. The mechanical properties are also crucial in contact lenses, as they determine the handling ability and cornea-lens coupling.

4.4. Thermal Properties. Thermostability of all membranes is around 280−290 °C and falls within the range of published studies.[13,46] This temperature indicates that they can be steam sterilized in standard conditions (121 °C and 1 pressure bar for 30 min) without decomposing. However, the secondary structure of the protein may be affected. The slight mass loss in the water and volatile molecule loss range (up to 200 °C) indicates that the membranes do not have high hygroscopic properties.

4.5. Topological Properties. The AFM analysis shows a rougher surface in membranes cross-linked with PEG. Previous literature also reported increased roughness with PEG and suggested that this is the result of PEG-induced phase separation.[44] Conversely, membranes cross-linked with methanol, ethanol, or isopropanol were stiffer and smoother. Membranes cross-linked with PEG, and subsequently treated with methanol, ethanol, or isopropanol, showed significantly reduced roughness compared to the PEG membrane alone. This may be due to the methanol, ethanol, or isopropanol treatment promoting crystallization into the β sheet conformation and increasing the organization of the SF structure.[47]

The ability, starting from the same SF solution, to control degradation, roughness, and stiffness offers great versatility in applications in the field of ophthalmology. For example, implants such as inlays or intraocular ring segments will benefit from long residency times conferred by long stability and nondegradability or breakage, while drug delivery applications will benefit from the possibility to modulate degradation. On the other hand, rougher membranes may be used as substrates or scaffolds, as cells have shown to grow better on rough surfaces.[28]

5. CONCLUSIONS

In conclusion, in this study, we report the protocols for extraction, casting, and cross-linking of SF from silkworms, in a detail seldom found in reports in the field. We provide a comprehensive evaluation of the stability, structural, topographical, mechanical, and optical properties, confirming that materials with a higher Young's modulus have a higher crystallinity, which also enhances the long-term stability of these materials. Besides, PEG induces roughness in the materials, increasing its water uptake.

The exhaustive control of the extraction and casting protocol guaranteed producing stable raw SF solution and a direct evaluation of the impact of the different cross-linking methods,

https://doi.org/10.1021/acsomega.4c02204
ACS Omega 2024, 9, 38452−38461

not contaminated by other factors. The versatility of the material properties achieved with processing opens up a breadth of applications. This work is meant to help potential users produce and select the material that best suits their needs, with a special focus but not exclusive, in ophthalmology applications.

■ ASSOCIATED CONTENT

Supporting Information

The Supporting Information is available free of charge at https://pubs.acs.org/doi/10.1021/acsomega.4c02204.

Transmittance of the materials in the 400−800 nm range; stress−strain curves of SF studied materials; FTIR spectra of the deconvoluted materials; SF secondary structure proportion in the materials; and TGA and DTG curves of all the studied materials (PDF)

■ AUTHOR INFORMATION

Corresponding Author

Rocio Gutierrez-Contreras − *Instituto de Óptica, Consejo Superior de Investigaciones Científicas (IO-CSIC), Madrid 28006, Spain; Universidad Politécnica de Madrid, Madrid 28040, Spain;* orcid.org/0000-0002-3849-3301; Email: rocio.gutierrez@csic.es

Authors

Mar Fernandez-Gutierrez − *Instituto de Óptica, Consejo Superior de Investigaciones Científicas (IO-CSIC), Madrid 28006, Spain;* orcid.org/0000-0003-1739-1987

Paula Olalla-Perez − *Instituto de Óptica, Consejo Superior de Investigaciones Científicas (IO-CSIC), Madrid 28006, Spain;* orcid.org/0009-0007-5588-2476

Andres De La Hoz − *Instituto de Óptica, Consejo Superior de Investigaciones Científicas (IO-CSIC), Madrid 28006, Spain;* orcid.org/0000-0003-0171-6433

Susana Marcos − *Instituto de Óptica, Consejo Superior de Investigaciones Científicas (IO-CSIC), Madrid 28006, Spain; Center for Visual Science, Flaum Eye Institute, Institute of Optics, University of Rochester, Rochester, New York 14642, United States;* orcid.org/0000-0001-5511-1697

Complete contact information is available at: https://pubs.acs.org/10.1021/acsomega.4c02204

Notes

The authors declare no competing financial interest.

■ ACKNOWLEDGMENTS

This work was supported by the European Research Council (2018-ADG-SILKEYE-833106). The authors would also like to thank the Optical Spectroscopies on Plasmonic and Semiconductor Nanostructures Group (IEM-CSIC) and the Laser Processing Group (IO-CSIC) for FTIR and transmittance measurements, respectively. They would also like to acknowledge Caleb Wigham, Juana Bellanato, Santiago Sanchez-Cortes and Ana Crespo-Solana for the very helpful discussions regarding FTIR spectra deconvolution, Pilar Posadas for assistance with AFM images, and Laura Barrios for assistance with statistical analysis.

■ REFERENCES

(1) Sun, W.; Gregory, D. A.; Tomeh, M. A.; Zhao, X. Silk fibroin as a functional biomaterial for tissue engineering. *Int. J. Mol. Sci.* **2021**, *22* (3), 1499.

(2) Mottaghitalab, F.; Farokhi, M.; Shokrgozar, M. A.; Atyabi, F.; Hosseinkhani, H. Silk fibroin nanoparticle as a novel drug delivery system. *J. Controlled Release* **2015**, *206*, 161−176.

(3) Marelli, B.; Brenckle, M. A.; Kaplan, D. L.; Omenetto, F. G. Silk Fibroin as Edible Coating for Perishable Food Preservation. *Sci. Rep.* **2016**, *6* (1), 25263.

(4) Pratap Singh, D.; Packirisamy, G. Biopolymer based edible coating for enhancing the shelf life of horticulture products. *Food Chem.: Mol. Sci.* **2022**, *4*, 100085.

(5) Wen, D. L.; Sun, D. H.; Huang, P.; Huang, W.; Su, M.; Wang, Y.; Han, M. D.; Kim, B.; Brugger, J.; Zhang, H. X.; et al. Recent progress in silk fibroin-based flexible electronics. *Microsyst. Nanoeng.* **2021**, *7* (1), 35.

(6) Rockwood, D. N.; Preda, R. C.; Yücel, T.; Wang, X.; Lovett, M. L.; Kaplan, D. L. Materials fabrication from Bombyx mori silk fibroin. *Nat. Protoc.* **2011**, *6* (10), 1612−1631.

(7) Koh, L. D.; Cheng, Y.; Teng, C. P.; Khin, Y. W.; Loh, X. J.; Tee, S. Y.; Low, M.; Ye, E.; Yu, H. D.; Zhang, Y. W.; et al. Structures, mechanical properties and applications of silk fibroin materials. *Prog. Polym. Sci.* **2015**, *46*, 86−110.

(8) Zhang, W.; Chen, L.; Chen, J.; Wang, L.; Gui, X.; Ran, J.; Xu, G.; Zhao, H.; Zeng, M.; Ji, J.; et al. Silk Fibroin Biomaterial Shows Safe and Effective Wound Healing in Animal Models and a Randomized Controlled Clinical Trial. *Adv. Healthcare Mater.* **2017**, *6* (10), 1−16.

(9) Nguyen, T. P.; Nguyen, Q. V.; Nguyen, V. H.; Le, T. H.; Huynh, V. Q. N.; Vo, D. V. N.; Trinh, Q. T.; Kim, S. Y.; Le, Q. V. Silk Fibroin-Based Biomaterials for Biomedical Applications: A Review. *Polymers* **2019**, *11* (12), 1933.

(10) Beena, M.; Ameer, J. M.; Kasoju, N. Optically Clear Silk Fibroin Films with Tunable Properties for Potential Corneal Tissue Engineering Applications: A Process-Property-Function Relationship Study. *ACS Omega* **2022**, *7* (34), 29634.

(11) Aznar-Cervantes, S. D.; Pagan, A.; Monteagudo Santesteban, B.; Cenis, J. L. Effect of different cocoon stifling methods on the properties of silk fibroin biomaterials. *Sci. Rep.* **2019**, *9* (1), 6703.

(12) Valles Ramirez, S. M.; De Moraes, M. A.; Beppu, M. M. Assessing the influence of silkworm cocoon's age on the physicochemical properties of silk fibroin-based materials. *J. Mater. Res.* **2019**, *34* (11), 1944.

(13) Wray, L. S.; Hu, X.; Gallego, J.; Georgakoudi, I.; Omenetto, F. G.; Schmidt, D.; Kaplan, D. L. Effect of processing on silk-based biomaterials: Reproducibility and biocompatibility. *J. Biomed. Mater. Res., Part B* **2011**, *99* (1), 89−101.

(14) Carissimi, G.; Lozano-Pérez, A. A.; Montalbán, M. G.; Aznar-Cervantes, S. D.; Cenis, J. L.; Víllora, G. Revealing the influence of the degumming process in the properties of silk fibroin nanoparticles. *Polymers* **2019**, *11* (12), 2045.

(15) Aznar-Cervantes, S. D.; Vicente-Cervantes, D.; Meseguer-Olmo, L.; Cenis, J. L.; Lozano-Pérez, A. A. Influence of the protocol used for fibroin extraction on the mechanical properties and fiber sizes of electrospun silk mats. *Mater. Sci. Eng., C* **2013**, *33* (4), 1945.

(16) Pritchard, E. M.; Hu, X.; Finley, V.; Kuo, C. K.; Kaplan, D. L. Effect of Silk Protein Processing on Drug Delivery from Silk Films. *Macromol. Biosci.* **2013**, *13* (3), 311.

(17) Um, I. C.; Kweon, H. Y.; Lee, K. G.; Park, Y. H. The role of formic acid in solution stability and crystallization of silk protein polymer. *Int. J. Biol. Macromol.* **2003**, *33* (4−5), 203.

(18) Kaewpirom, S.; Boonsang, S. Influence of alcohol treatments on properties of silk-fibroin-based films for highly optically transparent coating applications. *RSC Adv.* **2020**, *10* (27), 15913.

(19) Mu, X.; Sahoo, J. K.; Cebe, P.; Kaplan, D. L. Photo-crosslinked silk fibroin for 3d printing. *Polymers* **2020**, *12* (12), 2936.

(20) Motta, A.; Maniglio, D.; Migliaresi, C.; Kim, H. J.; Wan, X.; Hu, X.; Kaplan, D. L. Silk fibroin processing and thrombogenic responses. *J. Biomater. Sci. Polym. Ed.* **2009**, *20* (13), 1875.

(21) Reddy, N.; Yang, Y. Structure and properties of ultrafine silk fibers produced by Theriodopteryx ephemeraeformis. *J. Mater. Sci.* **2010**, *45* (24), 6617.
(22) Kaewpirom, S.; Boonsang, S. Optical and Structural Properties of Insoluble and Flexible Biodegradable Regenerated Silk Films for Optically Transparent Hydrophilic Coating of Medical Devices. *Adv. Mater. Interfaces* **2022**, *9* (9), 1−14.
(23) Bucciarelli, A.; Mulloni, V.; Maniglio, D.; Pal, R. K.; Yadavalli, V. K.; Motta, A.; Quaranta, A. A comparative study of the refractive index of silk protein thin fi lms towards biomaterial based optical devices. *Opt. Mater.* **2018**, *78*, 407.
(24) Hu, X.; Kaplan, D.; Cebe, P. Determining beta-sheet crystallinity in fibrous proteins by thermal analysis and infrared spectroscopy. *Macromolecules* **2006**, *39* (18), 6161.
(25) Lawrence, B. D.; Omenetto, F.; Chui, K.; Kaplan, D. L. Processing methods to control silk fibroin film biomaterial features. *J. Mater. Sci.* **2008**, *43* (21), 6967.
(26) Valente, F.; Allardyce, B. J.; Hepburn, M. S.; Wijesinghe, P.; Redmond, S. L.; Chen, J.; Kennedy, B. F.; Rajkhowa, R.; Atlas, M. D.; Wang, X.; et al. Enhancing Resistance of Silk Fibroin Material to Enzymatic Degradation by Cross-Linking Both Crystalline and Amorphous Domains. *ACS Biomater. Sci. Eng.* **2020**, *6* (4), 2459.
(27) Lawrence, B. D.; Wharram, S.; Kluge, J. A.; Leisk, G. G.; Omenetto, F. G.; Rosenblatt, M. I.; Kaplan, D. L. Effect of hydration on silk film material properties. *Macromol. Biosci.* **2010**, *10* (4), 393−403.
(28) Cheng, G.; Wang, X.; Song, C.; Zhang, X. Directly self-assembling method to easily prepare rough silk fibroin film. *Soft Mater.* **2022**, *20* (3), 251.
(29) Guo, C.; Li, C.; Kaplan, D. L. Enzymatic Degradation of Bombyx mori Silk Materials: A Review. *Biomacromolecules* **2020**, *21* (5), 1678.
(30) Cao, Y.; Wang, B. Biodegradation of silk biomaterials. *Int. J. Mol. Sci.* **2009**, *10* (4), 1514.
(31) Grabska-Zielińska, S.; Sionkowska, A. How to improve physico-chemical properties of silk fibroin materials for biomedical applications?—blending and cross-linking of silk fibroin—a review. *Materials* **2021**, *14* (6), 1510.
(32) Ratanasongtham, P.; Watanesk, R.; Watanesk, S. Comparison of porosity improvement of silk fibroin membrane using polyethylene glycol and glutaraldehyde for increasing oxygen permeability. *Adv. Mater. Res.* **2013**, *750−752* (August), 1601.
(33) Lu, S.; Wang, X.; Lu, Q.; Zhang, X.; Kluge, J. A.; Uppal, N.; Omenetto, F.; Kaplan, D. L. Insoluble and flexible silk films containing glycerol. *Biomacromolecules* **2010**, *11* (1), 143.
(34) Wang, Y.; Zheng, Z.; Cheng, Q.; Kaplan, D. L.; Li, G.; Wang, X. Ductility and Porosity of Silk Fibroin Films by Blending with Glycerol/Polyethylene Glycol and Adjusting the Drying Temperature. *ACS Biomater. Sci. Eng.* **2020**, *6* (2), 1176.
(35) Sterner, O.; Aeschlimann, R.; Zürcher, S.; Osborn Lorenz, K.; Kakkassery, J.; Spencer, N. D.; Tosatti, S. G. P. Friction measurements on contact lenses in a physiologically relevant environment: Effect of testing conditions on friction. *Investig. Ophthalmol. Vis. Sci.* **2016**, *57* (13), 5383.
(36) Hu, X.; Shmelev, K.; Sun, L.; Gil, E. S.; Park, S. H.; Cebe, P.; Kaplan, D. L. Regulation of silk material structure by temperature-controlled water vapor annealing. *Biomacromolecules* **2011**, *12* (5), 1686.
(37) Carissimi, G.; Baronio, C. M.; Montalbán, M. G.; Víllora, G.; Barth, A. On the secondary structure of silk fibroin nanoparticles obtained using ionic liquids: An infrared spectroscopy study. *Polymers* **2020**, *12* (6), 1294.
(38) Horcas, I.; Fernández, R.; Gómez-Rodríguez, J. M.; Colchero, J.; Gómez-Herrero, J.; Baro, A. M. WSXM: A software for scanning probe microscopy and a tool for nanotechnology. *Rev. Sci. Instrum.* **2007**, *78* (1), 013705.
(39) Koperska, M. A.; Pawcenis, D.; Bagniuk, J.; Zaitz, M. M.; Missori, M.; Łojewski, T.; Łojewska, J. Degradation markers of fibroin in silk through infrared spectroscopy. *Polym. Degrad. Stab.* **2014**, *105* (1), 185−196.
(40) Lu, Q.; Hu, X.; Wang, X.; Kluge, J. A.; Lu, S.; Cebe, P.; Kaplan, D. L. Water-insoluble silk films with silk I structure. *Acta Biomater.* **2010**, *6* (4), 1380.
(41) Lu, Q.; Zhang, B.; Li, M.; Zuo, B.; Kaplan, D. L.; Huang, Y.; Zhu, H. Degradation mechanism and control of silk fibroin. *Biomacromolecules* **2011**, *12* (4), 1080.
(42) Cheng, Y.; Koh, L. D.; Li, D.; Ji, B.; Han, M. Y.; Zhang, Y. W. On the strength of β-sheet crystallites of Bombyx mori silk fibroin. *J. R. Soc. Interface* **2014**, *11* (96), 20140305.
(43) Kling, S.; Marcos, S. Effect of hydration state and storage media on corneal biomechanical response from in vitro inflation tests. *J. Refract. Surg.* **2013**, *29* (7), 490.
(44) Suzuki, S.; Dawson, R.; Chirila, T.; Shadforth, A.; Hogerheyde, T.; Edwards, G.; Harkin, D. Treatment of Silk Fibroin with Poly(ethylene glycol) for the Enhancement of Corneal Epithelial Cell Growth. *J. Funct. Biomater.* **2015**, *6* (2), 345.
(45) Shen, G.; Hu, X.; Guan, G.; Wang, L. Surface modification and characterisation of silk fibroin fabric produced by the layer-by-layer self-assembly of multilayer alginate/regenerated silk fibroin. *PLoS One* **2015**, *10* (4), No. e0124811.
(46) Zhao, M.; Qi, Z.; Tao, X.; Newkirk, C.; Hu, X.; Lu, S. Chemical, thermal, time, and enzymatic stability of silk materials with silk i structure. *Int. J. Mol. Sci.* **2021**, *22* (8), 4136.
(47) Nogueira, G. M.; Rodas, A. C. D.; Leite, C. A. P.; Giles, C.; Higa, O. Z.; Polakiewicz, B.; Beppu, M. M. Preparation and characterization of ethanol-treated silk fibroin dense membranes for biomaterials application using waste silk fibers as raw material. *Bioresour. Technol.* **2010**, *101* (21), 8446.

https://doi.org/10.1021/acsomega.4c02204
ACS Omega 2024, 9, 38452−38461